

Fabrication of Inorganic Monolith Coated with Gold Nanoparticles for Protein Purification

Eman Alzahrani, Ahmed M Fallatah

Chemistry Department, Faculty of Science, Taif University, Taif, KSA

*E-mail: em-s-z@hotmail.com, a.fallatah.11@hotmail.com

Received: 2 September 2018 / Accepted: 4 November 2018 / Published: 5 January 2019

This work aims at developing a new technique used to fabricate porous inorganic monolith using pore surface improved coverage with gold nanoparticles (AuNPs) that has the capacity of preconcentrating proteins that has effectiveness of high preconcentration. The advantage of incorporating inorganic monolith with gold nanoparticles is getting high effective isolation of target analytes as a result of helpful features of surface area. Initially, the inorganic monolith was fabricated using the sol-gel process. The fabricated monolithic material was then chemically modified using 3-mercaptopropyltrimethoxysilane, and subsequently AuNPs immobilization on the surface of the inorganic monolith was performed. The materials that were synthesized were studied with the use of diverse methods such as FT-IR analysis, UV-Vis spectroscopy, EDAX and TEM analysis. As a fabricated sorbent for preconcentration of standard proteins (hemoglobin and pepsin), the AuNPs modified inorganic monolith was applied and its performance was contrasted with bare inorganic monolith. The fabricated AuNPs modified inorganic monolith would be a powerful sorbent for protein preconcentration from a real sample that is complicated.

Keywords: preconcentration, standard proteins, inorganic monolith, sorbent media, and gold nanoparticles.

1. INTRODUCTION

It is well-known that diverse stages of analytical techniques exist. These comprise data analysis, sampling, detection and sample preparation. The sample preparation's purpose is removal of meddlesome materials as well as preconcentrate of the interested analytes. Therefore, the interested sample's signal intensities will be enhanced, and the analyte quantities also can be measured easily [1-3].

The step of sample preparation is recognized as the most critical one because it is labor-intensive, time consuming and complex. An ideal sample preparation procedure should therefore be as simple as

possible, the procedure ought to be reproducible having the greatest target analytes' extraction recovery and should also be fast. Furthermore, it ought to necessitate potentiality of being used in on-line technique arrangement, lessen solvent consumption, the least number of processing steps and be environmentally friendly. The sample preparation step is therefore believed to be the analytical procedure's bottleneck. Consequently, the choice of a suitable procedure of sample preparation is a major factor in the analysis success, and if an unsuitable sample preparation method is applied, the whole analytical process can be squandered [4-6].

In general, sample preparation strategies can be classically derived from LLE (liquid-liquid extraction), or SPE (solid phase extraction). Despite the fact that LLE method is capable of offering high proficiency and low operation cost, the accessibility of diverse SPE sorbents materials is the main benefit over the LLE method. In addition, it is not possible to automate LLE, and necessitate large volumes of toxic solvents which are costly. When using LLE contrasted with SPE, it is possible to extract restricted number of samples. In accordance with these facts, SPE method is capable of overcoming LLE methods' limitations [7-9].

In SPE, the sorbent selection is the major factor, determined by the target analytes' properties, the kind of samples matrix, and the interfering materials that ought to be removed. For SPE, the ideal sorbent material to be applied must not be degraded by micro-organisms when biological sample is being used and it must not be influenced by storage or high temperature. The SPE sorbent has to be chemically stable and do not react with solvents. Furthermore, among the most essential properties of a suitable sorbent for SPE is a great surface area that is comparative to the sorbent's capacity with the aim of increasing its loadability [10, 11]. The SPE sorbent permeability is one more essential property of the sorbent used, with the aim of decreasing the processing time by reducing the backpressure and raising the rate of flow. Furthermore, an appropriate SPE sorbent should be capable of giving batch-to-batch reproducibility as well as separating undesired from desired components [8, 9].

Monolithic materials are the current materials which have been used as SPE sorbents. An organic and inorganic material is where these materials can be prepared from [10-14]. The inorganic monolithic materials have numerous benefits for instance high mechanical strength, high porosity, relatively high thermal stability and also organic solvents do not affect them. Inorganic monoliths have a distribution of both mesopores that can upsurge the surface area that allows a good interaction with analytes at the same time maximizes the sorbent loadability and macropores that can raise the flow of liquid through the monolith deprived of escalating the backpressure. The surface of an inorganic monolith has silanol groups (Si-OH) that can be applied in immobilizing diverse functional groups, as well as the groups' attachment on the inorganic surface beings easier as compared to an organic polymer support owing to its high number of crosslinking bonds which call for hours before reaching equilibrium, aimed at surface activation. In CEC (capillary electrochromatography), HPLC (high performance liquid chromatography) and GC (gas chromatography), synthetic inorganic monolithic materials have been presented as means of porous monolithic separation [15-17]. There are few papers that describe the use of inorganic monolith as materials for proteins extraction despite their increasing popularity as sorbents.

For a long period of time, AuNPs (gold nanoparticles) have been used. They are currently broadly used owing to their biological compatibility, molecular recognition as well as their special optical properties. AuNPs can also provide a large surface area to volume ratio with the aim of increasing the

relations with the analytes [18-20]. Despite the fact that AuNPs have been used in diverse fields and have been used to modify the materials' surface, it is only a few studies that can define AuNPs' application in the monolithic arena and fabrication. Furthermore, a technique that is more effective is needed to fabricate inorganic monolith using improved immobilized AuNPs' coverage. In this study therefore, we were able to prepare the inorganic monolithic matrix, then modification using mercapto groups. AuNPs decorated the mercapto functionalized inorganic monolith. The standard proteins (hemoglobin and pepsin) were preconcentrated with the use of the AuNPs-functionalized inorganic monolithic material.

2. EXPERIMENTAL

2.1. Materials and Chemicals

Polyethylene oxide (PEO) with the average relative molecular mass of RMM = 10000 Da, tetramethylorthosilicate 99% (TMOS), (3-mercaptopropyl)trimethoxysilane 95%, and standard pepsin and hemoglobin were purchased from Sigma-Aldrich (Poole, UK) and used as received without further purification. Gold(III) chloride trihydrate 99.8% ($\text{HAuCl}_4 \cdot 3\text{H}_2\text{O}$), phosphate-buffered saline (PBS), nitric acid, ammonia, toluene, acetone, sodium borohydride (NaBH_4), trifluoroacetic acid (TFA) and HPLC grade acetonitrile (ACN) were purchased from Fisher Scientific (Loughborough, UK). Distilled water was employed for preparing all the solutions and reagents. a Falcon™ conical centrifuge tube (50 mL) and polytetrafluoroethylene (PTFE) thread seal tape were purchased from ARCO Ltd. (Hull, UK). Disposable plastic syringes (1 mL) were purchased from Scientific Laboratory Supplies (Nottingham, UK).

2.2. Instrumentation

A hot plate-stirrer from VWR International LLC (West Chester, PA, USA). HPLC analysis was carried out using a Perkin Elmer LC200 series binary pump, a Symmetry C_{18} column, 4.6 mm \times 250 mm packed with silica particles (size 5 μm) from Thermo Fisher Scientific (Loughborough, UK) and a Perkin Elmer 785A UV/Visible Detector from Perkin Elmer (California, USA). pH meter Fisherman hydruS 300 from Thermo Orion (Beverly, MA, USA), TDL-5-A centrifuge from Anting Scientific Instrument Factory (Shanghai, China). Energy dispersive X-ray (EDAX) analysis was carried out using a INCA 350 EDAX system from Oxford Instruments (Abingdon, UK). The UV-Vis spectrophotometer was from Thermo Scientific GENESYS 10S (Toronto, Canada). The transmission electron microscopy (TEM) was from JEOL Ltd. (Welwyn Garden City, UK). The FT-IR spectra were PerkinElmer RX FTIR $\times 2$ with diamond ATR, and DRIFT attachment from PerkinElmer (Buckinghamshire, UK).

2.3. Mercapto-functionalised inorganic monolith fabrication

The polycondensation and hydrolysis of precursors synthesized the bare inorganic monolithic material with the use of a two-step sol-gel technique that succeeds the previously described procedure.

The fabrication of porous monolithic rod was through mixing of the following in a Falcon™ conical centrifuge tube (50 mL): 2.256 mL of TMOS, 0.282 g of PEO, 0.291 mL of distilled water and 2.537 mL of 1 M nitric acid solution. For a hydrolytic reaction to be promoted, the solution was aggressively agitated as it is being immersed in an ice bath until the two phase mixture steadily becoming a solution that is homogeneous.

Slowly, the acidified polymer solution was emptied into a 1 mL disposable plastic syringe, with internal diameter of 4.5 mm. The mixture was carefully shaken to eliminate any air bubbles when it was in the syringe. The syringe's thin end was sealed with the use of the PTFE thread seal tape. Consequently, the syringe was placed at 40 °C for 24 h in an oven. The wet inorganic monolith rod was afterwards slowly released from the plastic syringe. The monolithic rod was soaked in a water bath for 2 h at room temperature. The subsequent monolithic rod was treated with a basic environment, produced by the thermal decomposition of 1 M aqueous ammonia solution in a conical flask (100 mL) at high temperature of 85 °C for 24 hours. The rod was rinsed using distilled water with the aim of eliminating the ammonia solution is eliminated. The monolithic rod was subsequently dried in an oven for 24 h at a temperature of 40 °C, then another 24 hours at 100 °C. The rod was finally placed in an oven at a temperature of 500 °C for 2 hours.

The inorganic monolithic material's surface was chemically modified using mercapto groups through a reaction between (3-mercaptopropyl)trimethoxysilane and silanol groups on the inorganic monolith. This was performed through immersion of the synthesized monolithic rod in test tube together with a solution of 40 % (v/v) (3-mercaptopropyl) trimethoxysilane in the reaction medium (dried toluene) for 12 hours at a temperature of 100 °C. Through washing of the mercapto-bonded inorganic monolith using distilled water after salinization, the non-covalently bonded (3-mercaptopropyl) trimethoxysilane solution was flushed out.

2.4. *In-situ generation of AuNPs within monolith*

The preparation of nanoparticles was with the use of reducing reagent, NaBH₄, which was added to HAuCl₄·3H₂O (1 mM) and the ratio used was 1:1. [21]. The newly prepared mercapto-modified inorganic monolith was then added to the mixture and placed in oven at a 100 °C for 4 hours. The resultant black color monolith was finally washed using distilled water to make sure that gold ions in the monolith and the unanchored AuNPs are removed.

2.5. *Monolithic material characterization*

2.5.1. *UV-Vis spectrophotometer.*

During exposure to reducing reagent, the HAuCl₄ solution reduction was followed with ease through observation of the UV-Vis spectrum. 1 mL of sample solution was diluted with 1 mL of distilled water. The absorbance of the mixture was then measured with the use of a UV-Vis spectrophotometer and contrasted with absorbance of distilled water as a blank over the 350 to 800 nm range functioned at a 1 nm resolution.

2.5.2. TEM analysis

The determination of morphology of the prepared inorganic monolithic materials was through transmission of electron microscopy. The sample was placed onto the amorphous carbon-coated 200-mesh copper grid and given room for drying at ambient temperature, before scanning the grid.

2.5.3. EDAX analysis

With the use of energy dispersive X-ray (EDAX) analysis, elemental analysis was carried out for both the AuNPs-mercaptop functionalized inorganic monolith; the mercaptop functionalized inorganic monolith as well as the bare inorganic monolith.

2.5.4. FT-IR analysis

In the ATR (attenuated total reflectance) mode, the FT-IR spectra were collected with the use of a PerkinElmer RX FT-IR $\times 2$ instrument with DRIFT attachment from PerkinElmer, diamond ATR (Buckinghamshire, UK). The prepared materials' chemical functionality was recognized qualitatively with the use of FT-IR (Fourier transmission infrared spectroscopy). Spectra between 650 and 4000 cm^{-1} were documented.

2.6. Protein extraction

Through supersonic adhesion, the fabricated monolithic rod was cut before being fixed into centrifugal spin column of 0.5 mL. Consequently, the spin column was fastened to the waste fluid tube. In protein preconcentration, this is the home-made spin column tube that was applied. The standard proteins (hemoglobin and pepsin) were preconcentrated through amendment of the technique previously established [22-25]. Preactivation of the sorbent was with ACN (0.1% TFA) solution (250 μL) using centrifuging at 1500 rpm for 2 minutes. The waste fluid was then eliminated from the waste fluid tube. Consequently, the monolithic material was equilibrated using ACN (250 μL) through centrifugation at 1500 rpm for 2 minutes, followed by eliminating the waste fluid from the waste fluid tube. 350 μL of standard protein solution (40 μM) that was dissolved in 50 mM tris-HCl buffer solution of pH 7.0 was loaded onto the spin column that is conditioned, prior to centrifugation at 1500 rpm for 3 minutes. Once loading of the protein standard was complete, the sorbent was washed using 150 μL of 50 mM tris-HCl (pH 7.0) through centrifugation, and then the waste fluid was eliminated from the waste fluid tube. The column was finally set up into a new microtube, then the retained protein was eluted using 60 % ACN (0.1 % TFA) solution (200 μL) through centrifugation at 1500 rpm for 2 minutes and the eluted protein was collected. All experiments were performed at an ambient temperature of approximately 23 °C. After every cycle, the monolith was washed using water and acetone, and then dried for 6 hours at 40 °C before the succeeding cycle is presented.

Under isocratic conditions, the eluent was directly injected into the HPLC-UV instrument and the mobile phase was acetonitrile-purified water (50:50). The sample injection volume was 20 μL . The rate of flow was set at 1 mL min^{-1} , 280 nm wavelength, and all experiments were carried out at an ambient temperature around 23 $^{\circ}\text{C}$. For evaluation of the proteins' extraction efficiency, ER (extraction recovery) was computed. Equation (1) is an illustration of the ER (extraction recovery) [33-35], described as the percentage of the total proteins amount that was being pulled out to the eluent:

$$ER = \left[\frac{C_{elu} \times V_{elu}}{C_{elu} \times V_{eq}} \right] \times 100 \quad (1)$$

Whereby C_{elu} and C_{elu} were acquired from the peak area attained with the solid phase extraction and deprived of purification, V_{eq} and V_{elu} represents the volumes of sample solution and eluent correspondingly.

3. RESULTS AND DISCUSSION

3.1. Characterization of AuNPs-mercapto functionalised monolith

It is well-known that the gold(III) chloride trihydrate's reduction into AuNPs normally followed by change of color as well as the formation of AuNPs can be observed visually [2, 26]. Color change therefore was monitored visually with the aim of checking for the AuNPs formation, as clearly illustrated in Figure 1.



Figure 1. Photos show tubes containing mixture of reducing reagent (NaBH_4) and HAuCl_4 solution (50:50); before (left), and after adding the inorganic monolith (right), showing changed the colour of the monolithic rod from white to black after incubation in oven at 100 $^{\circ}\text{C}$ for 4 h.

It was observed that the HAuCl_4 solution's yellow color was changed to black after the reducing reagent was added. The black colour was as a result of the of surface plasmon vibrations' excitation in the gold nanoparticles [27]. It was also observed that when incubation of the monolithic rod in the

mixture of reducing reagent and HAuCl_4 solution for 4 hours in oven at very high temperature of $100\text{ }^\circ\text{C}$, the mixture solution's black color was decreased as the monolithic rod's colour was turned to black from white, brought about by the inorganic monolithic rod's functionalization with AuNPs.

The dried crack-free inorganic monolithic rod after and before coating with AuNPs is clearly illustrated in Figure 2. It was observed that the bare inorganic monolithic rod's color was bright white, Figure 2 (left), then the bare inorganic monolithic rod's color changed to black owing to the coating of metallic nanoparticles on the mercapto-modified inorganic monolith, on the right Figure 2, and the colour was not altered after the monolithic rod was washed using distilled water so that gold ions and the unbounded AuNPs are eliminated.



Figure 2. The appearance of the dried inorganic monolith (left), and AuNPs-embedded inorganic monolith (right).

Because AuNPs are capable of absorbing light in the visible region as a result of the surface Plasmon resonance phenomenon according to their shape and size [27, 28], the prepared solutions' UV-Vis spectra were examined with the use of UV-V refer to spectrophotometer. An illustration of contrast between AuNPs colloidal solution and the UV-Visible absorption spectra of AuNPs colloidal solution, after the inorganic monolithic rod has been added is in Figure 3. It was observed from the spectra that the fabricated AuNPs had a maximum absorbance peak as a result of the gold ions reduction to colloidal AuNPs [29, 30]. After the monolithic rod was added to the mixture, it was discovered that there was a substantial reduction in the AuNPs colloidal solution's absorbance strength. The AuNPs's formation as well as the anchor of the formed_AuNPs to the pore surface of the inorganic monolithic rod after monolithic rod was added in the solution was confirmed by the UV-Vis spectra.

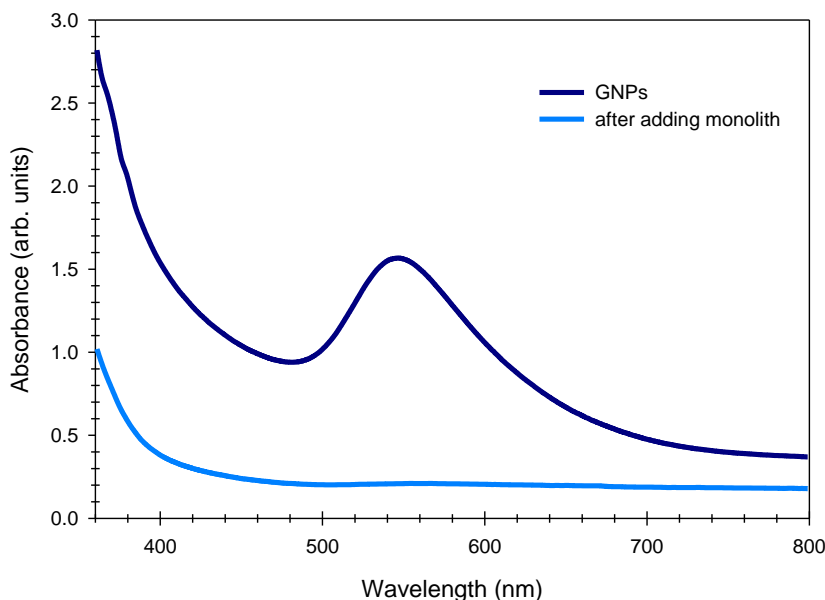


Figure 3. Comparison between the UV-Vis absorption spectra of AuNPs colloidal solution, and AuNPs colloidal solution after adding the inorganic monolithic rod. 1 mL of sample solution was diluted with 1 mL of distilled water. The absorbance of the mixtures were measured using a UV-Vis spectrophotometer, and the absorbance of distilled water was also measured as a blank over the range of 350 to 800 nm that was operated at a resolution of 1 nm.

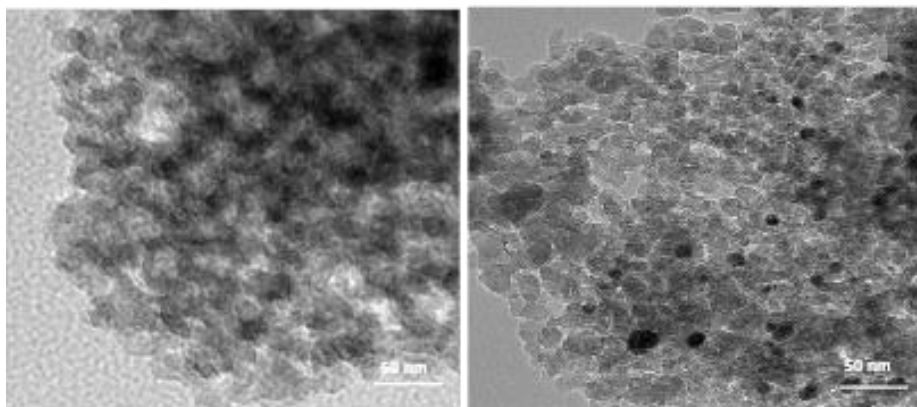


Figure 4. TEM images of bare inorganic monolith (left), and AuNPs-embedded inorganic monolith (right).

The AuNPs that was formed immobilized mercapto group-modified macroporous inorganic monolith were investigated with the use of TEM analysis. In Figure 4, there is clear illustration of TEM electron microscopy micrographs of inorganic monolithic materials before, on the left side of Figure 4, and after immobilization of AuNPs on the inorganic monolith materials' surface, on the right side of Figure 4. Through the comparison of the micrographs, it is clear that at the pore surface of the mercapto

group-modified monolith (dark spots) AuNPs were immobilized, suggesting that AuNPs were effectively immobilized on the mercapto modified inorganic monolith. It was discovered in this study that there was no AuNPs' aggregation as a result of the existence of mercapto moieties that inhibit aggregation, resulting in a particle size dissemination that is more constant.

With the use of EDAX analysis, the synthesized monoliths were further studied with the aim of identifying the chemical composition of the synthesized materials. The EDAX spectra between 0 keV and 10 keV of bare inorganic monolith, above, and AuNPs-mercapto modified inorganic monolith, bottom, is well illustrated in Figure 5. It can be perceived from the images that the bare inorganic monolith's EDAX image presented strong peaks for Si and O. In the EDAX spectrum of AuNPs-mercapto modified inorganic monolith, it was observed that beside the peaks for the C, O and Si, which is a new peak at 2.123 keV was discovered, which was interrelated to Au element, endorsing the effective immobilization of AuNPs on the mercapto modified inorganic monolith's surface.

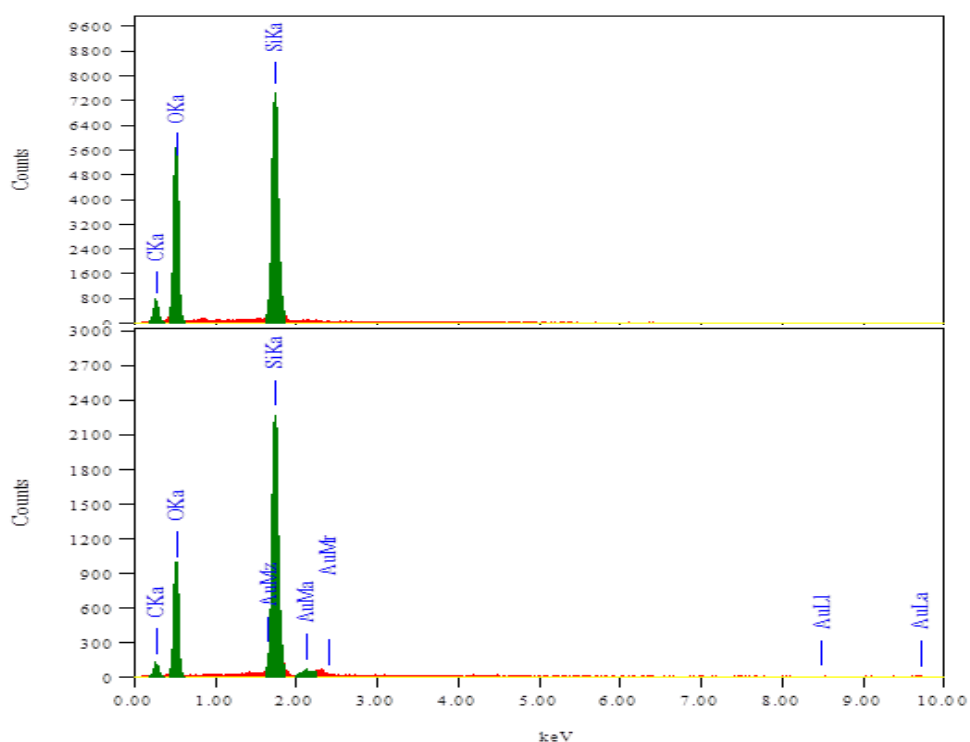


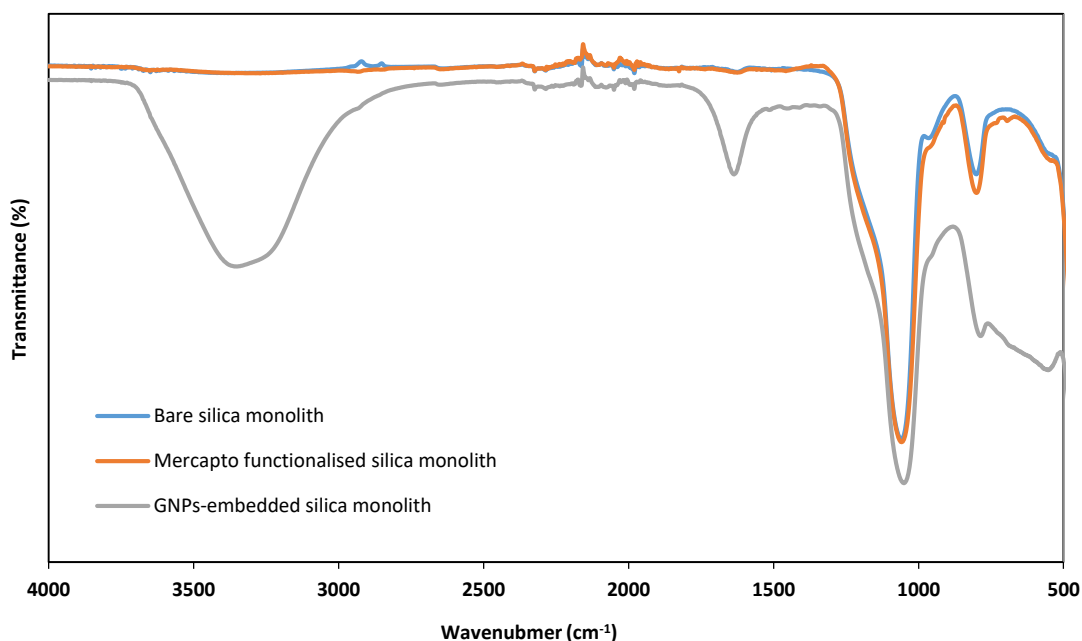
Figure 5. EDAX spectra of bare inorganic monolith (above), and AuNPs- mercapto modified inorganic monolith (bottom).

The composition of 22.81% Si, 10.54% C and 66.65% O in inorganic monolith is presented in Table 1. Alongside Si, C and O however, 2.08% S was realized in the mercapto modified inorganic monolith, which confirmed the inorganic monolith's surface modification. In addition, in the fabricated monolithic material encrusted with gold nanoparticles, there is 2.82 % of Au deprived of any rudimentary impurities.

Table 1. elemental composition of the fabricated materials determined by energy-dispersive X-ray analysis.

Sample	Atom%					Total
	C	O	Si	S	Au	
Bare inorganic monolith	10.54	66.65	22.81	0	0	100
Modified inorganic monolith with mercapto groups	18.45	53.86	25.61	2.08	0	100
GNPs embedded inorganic monolith	14.62	54.51	26.92	1.13	2.82	100

For the chemical structure changes between the bare and modified inorganic monolith with mercapto groups to be further investigated, and further AuNPs' immobilization at the same time approval of the mercapto moieties' grafting on the inorganic monolith's surface, Fourier transform infrared (FT-IR) spectroscopy was used, due to the fact that this method is capable of following structural alterations that took place at the surface as well as in the inorganic monolith's network [31]. Figure 6 shows the FT-IR spectra of the bare silica inorganic monolith, blue spectrum, after the surface of the inorganic monolith with mercapto groups have been modified, red spectrum, as well as after immobilization of AuNPs in monolithic material, green spectrum.

**Figure 6.** FT-IR spectra of the bare inorganic monolith (blue spectrum), the mercapto modified inorganic monolith (red spectrum), and SNPs functionalized mercapto group inorganic monolith (green spectrum). The IR range was in the middle infrared range (500-4000 cm^{-1}) using 6 scans at a resolution of 4 cm^{-1} .

As well illustrated in the figure, a robust band situated at around 1075 cm^{-1} matched to asymmetric stretching vibration of Si-O-Si, an indication of a robust framework that is cross-linked. The band approximately 784 cm^{-1} stemmed from symmetric stretching vibration of Si-O-Si. For the two samples, these two bands of the inorganic frameworks were detected. At 3300 cm^{-1} , 1600 cm^{-1} , 660 cm^{-1} to 560 cm^{-1} , prominent peaks for the AuNPs mercapto-functionalized inorganic monolith were detected. The extreme witnessed at 3300 cm^{-1} is an implication of the presence of a hydrogen bond whereas the highest at 1600 cm^{-1} could be accredited to C=C, stretching mode. The peaks to 560 cm^{-1} from 660 cm^{-1} might be brought about by OH groups' wagging mode [32-34]. The FT-IR outcomes approve that AuNPs incrustated the monolithic materials.

3.2. Preconcentration of proteins

The study's objective was to compare the performance of AuNPs-mercapto functionalised inorganic monolith with inorganic monolith to be used in extraction of protein with the aim of identifying the one that is more operational to be applied as SPE (solid phase extraction) sorbent. The handling of conventional SPE cartridges is easy with the use of a positive-pressure manifold or a vacuum. It is however not easy to regulate the rate of flow, and care ought to be taken with the aim of preventing the drying out of a column before sample application[35]. The rate of flow on the other hand could be regulated easily only through observation of the rotation speed of centrifuge along with the inaccuracies related to handling of sample in spin columns are significantly small in relation to other formats of micro extraction like pipette tips; as a result, the centrifuge was applied in injecting the sample. The fabricated monolithic materials were applied in preconcentration of standard proteins that were hemoglobin and pepsin. The standard proteins' concentration was $40\text{ }\mu\text{M}$ and it was prepared in 50 mM tris-HCl buffer solution (pH 7).

The monolithic disk was fixed into cartridge spin column, then the spin column was attached to the waste fluid tube [23, 36]. As described in section 2.6, the preconcentration steps, comprise activation with ACN (0.1 % TFA) solution ($250\text{ }\mu\text{L}$) so that impurities are removed and before being equilibrated using ACN ($250\text{ }\mu\text{L}$) to equilibrate the monolith as well as guarantee protein peak binding. After the monolithic material in the spin column is equilibrated, the sample solution was used ($350\text{ }\mu\text{L}$), then the monolithic disk was washed with the use of $150\text{ }\mu\text{L}$ of 50 mM tris-HCl (pH 7.0). The preconcentrated protein was finally eluted using 60 % ACN (0.1 % TFA) solution ($200\text{ }\mu\text{L}$) and the eluate investigated using HPLC-UV instrument. The optimal centrifugation speed needed for good recovery appeared to be 1500 rpm, the process of extraction was not so time wasting, and the column did not dry out, hence accomplishment of good analyte recovery.

The monolithic rod's performance that SNPs had not modified was compared with monolithic rod had SNPs. The rationale behind retention of the proteins was the interaction between the functional groups of the protein and the AuNPs on the surface of the inorganic monolithic materials. In Figure 7, there is illustration of hemoglobin chromatograms with the use of direct inject of standard protein (a), after applying bare inorganic monolith (b), as well as after applying AuNPs implanted inorganic monolith (c). Through comparison of the peak area of standard hemoglobin, deprived of preconcentration, with ultimate area of purified hemoglobin with bare inorganic monolith as well as with

inorganic monolith reformed with the use of AuNPs, it was found that the highest peak of hemoglobin was attained when AuNPs implanted monolith was applied. Consequently, the analysis' sensitivity was enhanced. Similar outcome was acquired when pre-concentrated pepsin applied the same material, as illustrated in Figure 8. This outcome is a confirmation of the capacity of the metal nanoparticles entrenched inorganic monolith with the aim of pre-concentrating standard proteins.

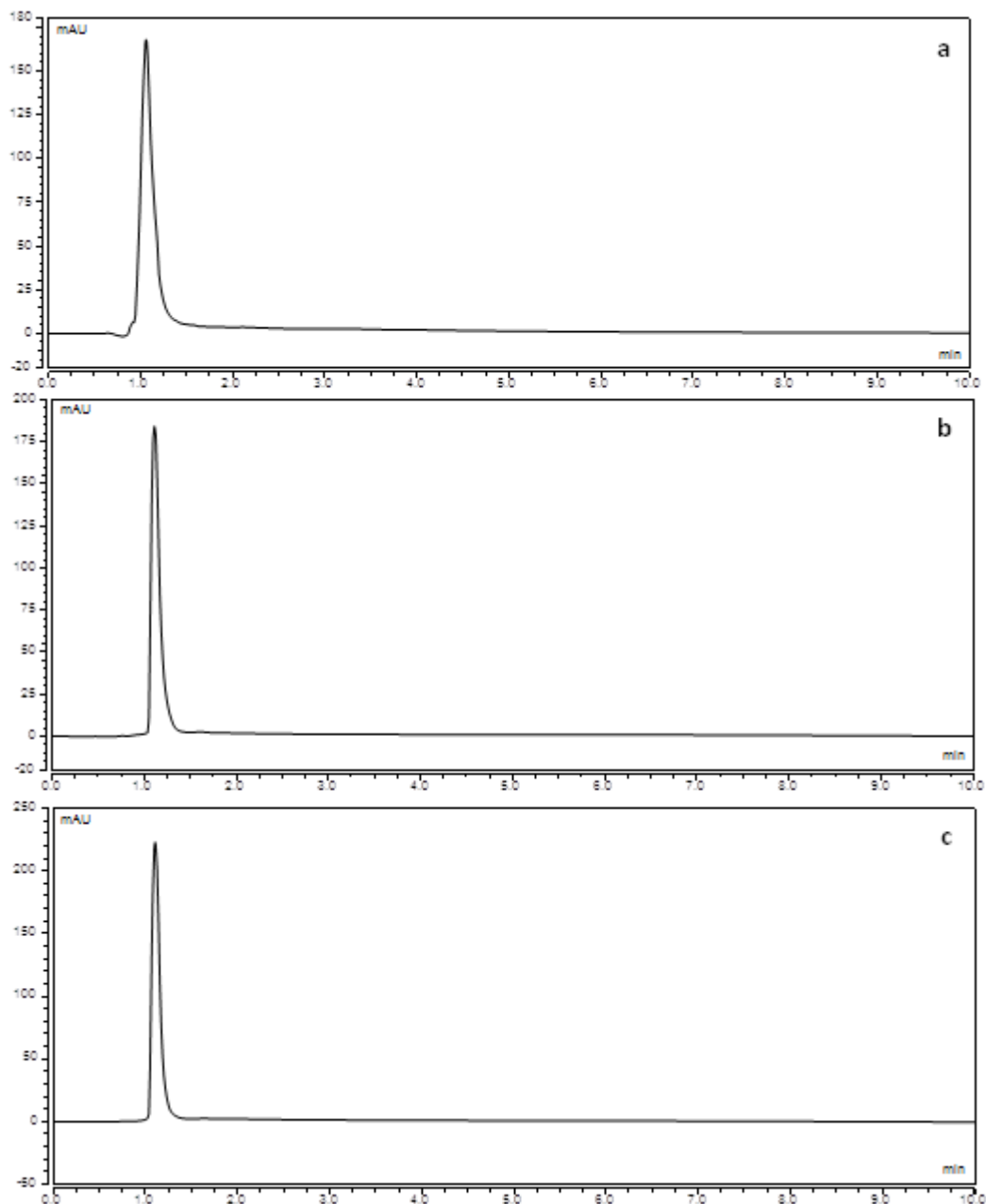


Figure 7. The difference in the UV chromatogram (a) 40 μ L of hemoglobin, (B) after extraction using bare inorganic monolith, and (c) after extraction using AuNPs embedded inorganic monolith.

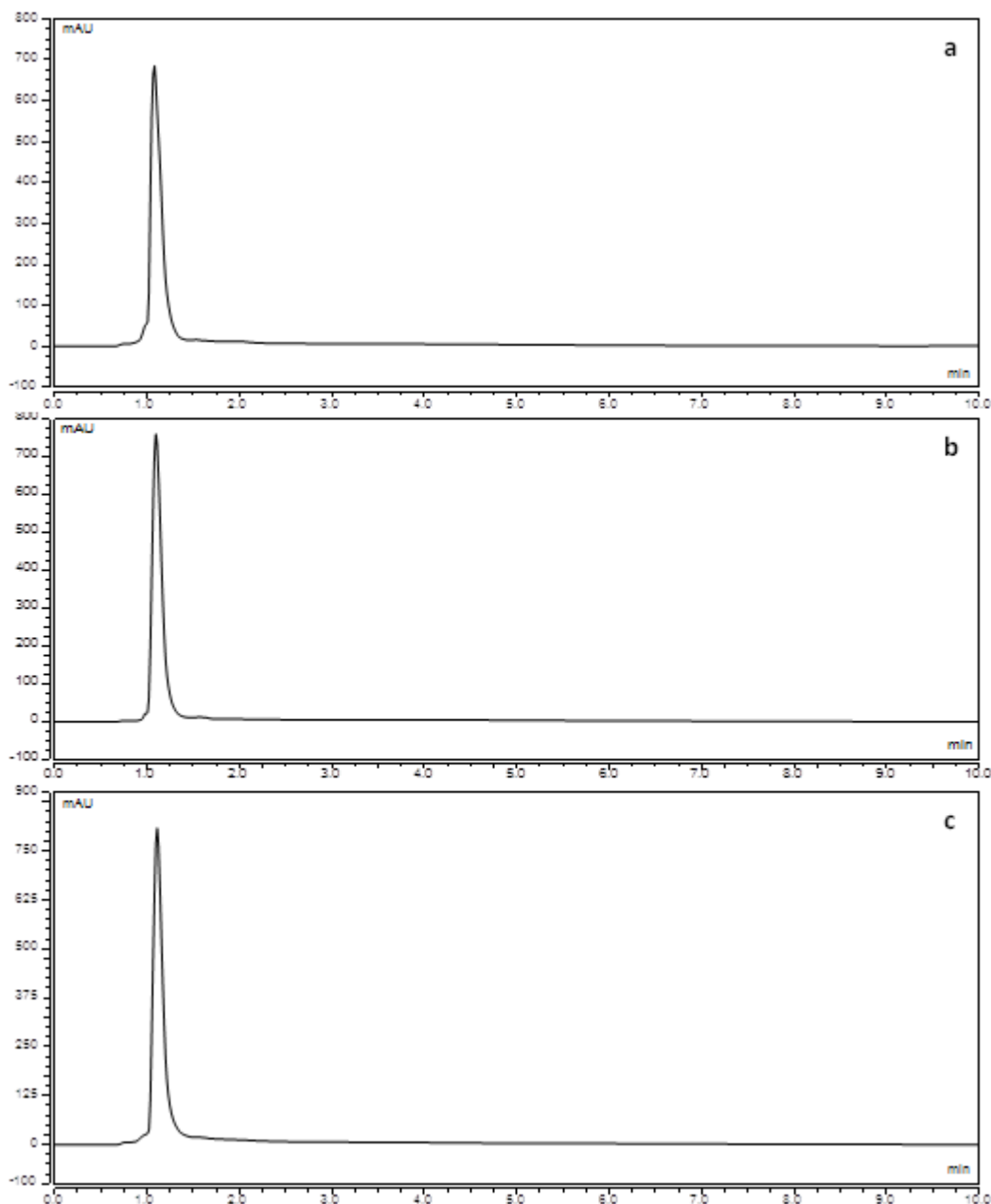


Figure 8. The difference in the UV chromatogram (a) 40 μ L of pepsin, (B) after extraction using bare inorganic monolith, and (c) after extraction using AuNPs embedded inorganic monolith.

The AuNPs' performance implanted inorganic monolith was compared with the one of bare inorganic monolith. The preconcentration of proteins was also performed under similar conditions. Table 2 clearly illustrates that the ER (extraction recovery) of purified proteins was computed from the UV chromatogram with the aim of comparing the performance of the fabricated AuNPs entrenched inorganic monolith with the bare inorganic monolith. The Table is an implication that it is possible to achieve a higher extraction efficiency with the use of AuNPs embedded inorganic monolith, 95 % and 90 % for

pepsin and hemoglobin, correspondingly, which is more enhanced as compared to the inorganic monolith, the extraction recoveries for pepsin and hemoglobin were 85 % and 74 % , respectively.

Table 2. Comparison of the extraction recoveries of the standard proteins purified with bare inorganic monolith and AuNPs embedded inorganic monolith.

Sample	Type of sorbent	Molecular mass (Da)	Isoelectric point (pI)	Extraction recovery (ER, %)
Hemoglobin	Bare inorganic monolith	64500	7.4	74
	AuNPs embedded inorganic monolith			90
Pepsin	Bare inorganic monolith	34620	3.2	85
	AuNPs embedded inorganic monolith			95

Although the performance of the inorganic monolith coated with gold nanoparticles for protein purification was better than the performance of bare silica monolith, it was found that the performance of AuNPs-functionalized inorganic monolithic material was lower than the performance of inorganic monolith coated with octadecylsilyl (C₁₈) groups since the extraction recovery of hemoglobin was 94.8% when using octadecylated inorganic monolith [3], which is more enhanced as compared to the inorganic monolith coated with gold nanoparticles (90%). The reason for that could be the hydrophobicity of octadecylsilyl groups on the surface of the inorganic materials is higher than the hydrophobicity of gold nanoparticles resulting in improve the inorganic monolith for protein purification.

3.3. Reproducibility of the fabricated materials

The reproducibility of the AuNPs embedded inorganic monolith's synthesis is a major factor when it comes to the practicality and efficiency of the procedure. This is due to the fact that the synthesis of the AuNPs embedded inorganic monolith a process that is multi-step. The reproducibility of the surface modification of the monolith is also a very vital prerequisite for approval of the used preparation technique, in industrial laboratories particularly [38]. Because of the high cost of fabrication, reusability is one of the most significant features of applying a fabricated material. The fabrication method's reproducibility was studied for three monoliths fabricated from three diverse mixtures with the use of similar procedure. The assessment of the reproducibility of synthesis of materials was done by checking the morphology illustrated by TEM for three diverse fabricated monolithic materials' batches had gold nanoparticles. It was discovered that there was a difference that is nonvisible in the morphology of the prepared monolithic materials had gold nanoparticles. The performance's reproducibility of the produced material was tested through computation of the relative standard deviation for the ER (extraction recovery) of the preconcentrated standard proteins. In Figure 9, there is clear an assessment of the extraction recovery (ER) of the preconcentrated standard proteins with the use of similar monolith, 3 runs, as well as the use of diverse monolith, n = 3. The results obtained from this study is an illustration that the preconcentrate standard proteins' procedure was reproducible since noble run-to-run

reproducibility was accomplished using RSD value that is below 2.5 %, whereas for batch-to-batch reproducibility, RSD value was below 6 percent.

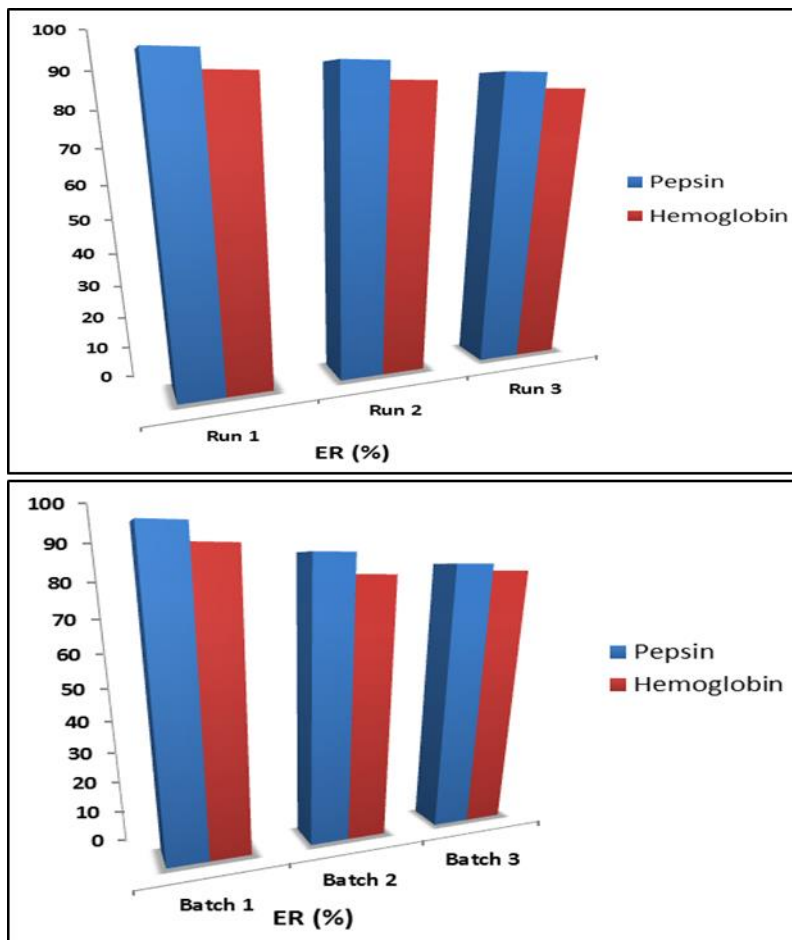


Figure 9. Comparison of the extraction recovery (ER) of the pre-concentrated standard proteins showing: The run-to-run reproducibility (above) and batch-to-batch reproducibility of the AuNPs embedded inorganic monolith (bottom).

Different various nanomaterials were utilized with different compositions and morphologies have been used as sorbents for the purpose of sample preparation, aiming for the enrichment or pre-concentration of target analytes or cleanup of the samples. Preconcentration is a crucial step in processing protein analysis, because of the complexity of the protein samples and the presence of different components in the same sample [37]. Considering silica monolith used in this work as an SPE tool for preconcentration and purification of protein analytes of interest from matrices. As there is a limited choice of silica monolith as a sorbents for extraction of protein; therefore, it is hard to find in the literature similar work to compare the results obtained in this work with previous studies.

4. CONCLUSION

Immobilization of AuNPs on the mercapto modified inorganic monolith in this study was carried out using a simple technique. This was accomplished through modification of the surface of inorganic silica monolith with mercapto moieties groups before the in situ AuNPs' fabrication, which was fabricated through the reduction of an inorganic precursor $\text{HAuCl}_4 \cdot 3\text{H}_2\text{O}$ with the use of NaBH_4 as the reducing reagent, along the monolith. The fabricated materials were placed in a spin column to be applied as sorbent. For preconcentration of standard proteins, the fabricated monolith was utilized and better performance was experienced as compared to that of bare inorganic monolith. This material is also cost-effective because the standard proteins can be extracted with the use of a small solvent volume. The capacity to fabricate with ease as well as use is an indication of this monolith's great prospective for protein preconcentration from actual sample.

ACKNOWLEDGEMENT

The authors are very grateful to Taif University, Taif, KSA, since this work was financially supported by Taif University, Taif, KSA, under project number 1/438/5573.

Reference

1. A. Kulakowska, A. Krzysik, T. Dylag, A. Drabik, P. Suder, M. Noga, J. Jarzebinska, J. Silberring, *J. Chromatogr. B*, 849(2007) 1.
2. E. Alzahrani, K. Welham, *Anal. Chim. Acta*, 798 (2013) 40.
3. E. Alzahrani, *Res. J. Pharm. Bio. and Chem. Sci.*, 7(2016)158.
4. G. Vas, K. Vekey, *J. Mass Spectrom.*, 39(2004) 233.
5. M. de Fatima Alpendurada, *J. Chromatogr. A*, 889(2000)
3. E. Alzahrani, K. Welham, *Analyst*, 137(2012) 4751.
7. R. N. Xu, L. Fan, M. J. Rieser, T. A. El-Shourbagy, *J. Pharm. Biomed. Anal.*, 44(2007) 342.
8. M. Gilar, E. S. Bouvier, B. J. Compton, *J. Chromatogr. A*, 909(2001) 111.
9. M. C. Hennion, *J. Chromatogr. A*, 856(1999) 3.
10. F. Svec, C. G. Huber, *Monolithic Mater: promises, challenges, achievements*. 2006, ACS Publications.
11. F. Svec, *J. Chromatogr. B*, 841(2006) 52.
12. E. Alzahrani, K. Welham, *Analyst*, 136(2011) 4321.
13. V. F. Samanidou, E. G. Karageorgou, *J. Sep. Sci.*, 34(2011) 2013.
14. J. Urban, *J. Sep. Sci.*, 39(2016) 51.
15. I. Azzouz, A. Essoussi, J. Fleury, R. Haudebourg, D. Thiebaut, J. Vial, *J. Chromatogr. A*, 1383(2015) 127.
16. F. Svec, E. C. Peters, D. Sýkora, C. Yu, J. M. J. Fréchet, *J. High Resolut. Chromatogr.*, 23(2000) 3.
17. W. Li, D. P. Fries, A. Malik, *J. Chromatogr. A*, 1044(2004) 23.
18. M. C. Daniel, D. Astruc, *Chem. Rev.*, 104(2004) 293.
19. X. Huang, P. K. Jain, I. H. El-Sayed, M. A. El-Sayed, *Nanomedicine*, 2(2007) 681.
20. Y. C. Yeh, B. Creran, V. M. Rotello, *Nanoscale*, 4(2012) 1871.
21. E. Alzahrani, *World J. Nano Sci. and Eng.*, 5(2015) 10.
22. M. Vergara-Barberán, M. García, E. Simó-Alfonso, J. Herrero-Martínez, *Anal. Chim. Acta*, 917(2016) 37.

23. T. Saito, R. Yamamoto, S. Inoue, I. Kishiyama, S. Miyazaki, A. Nakamoto, M. Nishida, A. Namera, S. Inokuchi, *J. Chromatogr. B*, 867(2008) 99.
24. A. Nakamoto, M. Nishida, T. Saito, I. Kishiyama, S. Miyazaki, K. Murakami, M. Nagao, A. Namura, *Anal. Chim. Acta*, 661(2010) 42.
25. M. Tsunoda, C. Aoyama, S. Ota, T. Tamura, T. Funatsu, *Anal. Methods*, 3(2011) 582.
26. V. Sarsar, K. K. Selwal, M. K. Selwal, *J. Microbiol. Biotechnol. Res.*, 3(2017) 27.
27. E. Alzahrani, *Anal. Chem. insights*, 12(2017)1.
28. X. Ding, C. H. Liow, M. Zhang, R. Huang, C. Li, H. Shen, M. Liu, Y. Zou, N. Gao, Z. Zhang, Y. Li, Q. Wang, S. Li, J. Jiang, *J. Am. Chem. Soc.*, 136(2014)15684.
29. D. Bose, S. Chatterjee, *Appl. Nanosci.*, 6(2016) 895.
30. S. G. Yadav, S. H. Patil, P. Patel, V. Nair, S. Khan, S. Kakkar, A. D. Gupta, *Int. J. Sci Res. Sci. Technol.*, 5(2018) 133.
31. D. Rivera, J. M. Harris, *Anal. Chim. Acta*, 73(2001) 411.
32. S. Chandran, V. Ravichandran, S. Chandran, J. Chemmunda, B. Chandarshekar, *J. Appl Res. Technol.*, 14(2016) 319.
33. S. Agnihotri, S. Mukherji, S. Mukherji, *Appl. Nanosci.*, 2(2012) 179.
34. K. Cheng, Y. Hung, C. Chen, C. Liu, J. Young, *Carbohydr. Polym.*, 110(2014) 195.
35. A. Namera, A. Nakamoto, M. Nishida, T. Saito, I. Kishiyama, S. Miyazaki, M. Yahata, M. Yashiki, M. Nagao, *J. Chromatogr. A*, 1208(2008) 71.
36. L. Lu, Y. Hashi, Z. Wang, Y. Ma, J. Lin, *J. Pharm. Anal.*, 1(2011) 92.
37. M. Ahmadi, H. Elmongy, T. Madrakian, M. Abdel-Rehim, *Anal. Chim. Acta*, 958 (2017) 1.

© 2019 The Authors. Published by ESG (www.electrochemsci.org). This article is an open access article distributed under the terms and conditions of the Creative Commons Attribution license (<http://creativecommons.org/licenses/by/4.0/>).